Scripta Materialia 134 (2017) 100–104

Contents lists available at ScienceDirect

Scripta Materialia

journal homepage: www.elsevier.com/locate/scriptamat

Regular Article

# High thermoelectric performance of BiCuSeO prepared by solid state reaction and sol-gel process

Ankam Bhaskar, Rung-Ting Lai, Kuo-Chuan Chang, Chia-Jyi Liu *

*Department of Physics, National Changhua University of Education, Changhua 500, Taiwan*

ARTICLE INFO

*Article history:*
Received 4 January 2017
Accepted 20 February 2017
Available online xxxx

*Keywords:*
Sol-gel
Hot pressing
Transmission electron microscopy
Thermoelectric materials
Thermal conductivity

ABSTRACT

BiCuSeO was synthesized by the conventional solid state reaction and the sol-gel method for comparative studies. The transport properties can be described using the single parabolic band with the assumption of acoustic phonon scattering as the dominant scattering mechanism. It is found that the material parameters depend on the synthesis procedures. The reduced Fermi energy of the sol-gel samples shifts to a position closer to the valence band edge as a result of an increase in carrier concentration. As a result, the power factor and *zT* of sol-gel sample is significantly enhanced as compared to the solid state reaction sample.



## 1. Introduction

According to the statistics released by International Energy Agency [1], the energy crisis is a serious problem for coming generation due to decreasing fossil fuels. Thermoelectricity is one of the potential solutions to provide green energy. Oxide thermoelectric materials are one of the potential candidates for a wide range of high temperature applications [2–5], such as layered cobalt oxides [6–8], perovskites [9], and simple oxides etc. [10–11]. However, the figure of merit (*zT*) is still at a relatively low level for industrial applications. Recently, the BiCuSeO system attracts much attention due to its higher *zT* value among the oxide thermoelectric materials [12–14]. The solid state reaction is a simple process, but it requires a high sintering temperature or prolonged firing time to form single phase. It is well known that chemical routes, especially sol-gel synthesis, avoid these problems. Therefore, sol-gel synthesis is adopted to prepare the BiCuSeO system. To the best of our knowledge, there is no report in the literature regarding BiCuSeO synthesized by the sol-gel method. In this study, we compare the effects of synthesis procedures on thermoelectric properties by synthesizing BiCuSeO by the conventional solid state reaction and the sol-gel method.

## 2. Experiments

Regarding the synthesis of the BiCuSeO samples, there are two methods adopted in the present study: the sol-gel method and the solid state reaction. As for the sol-gel method, $Bi(NO_3)_3 \cdot 5H_2O$, $Cu(NO_3)_2 \cdot 5H_2O$, Se powders were quantitatively dissolved in deionized water with the solution stirring at 60 rpm. Citric acid ($C_6H_8O_7$) and ethylene glycol ($C_2H_8O_2$) were added into the solution in appropriate proportions. The solution was heated to 95 °C to allow the polymerization reaction to occur and form the gel. The gel was then dried at 80 °C for 8 h. The dried powders were divided into two batches for calcination, followed by consolidation using hot pressing. One batch (sample SGA) of powders were directly heated to 550 °C with a ramp rate of 2.5 °C/min and kept for 12 h in flowing $N_2$ atmosphere, followed by cooling to room temperature at 2.5 °C/min. The calcined powders were hot pressed with an applied pressure of 80 MPa at 580 °C for 30 min., followed by furnace cooling to room temperature. The second batch (sample SGB) of powders were first heated to 250 °C with a ramp rate of 1 °C/min and kept for 2 h, and then to 550 °C with a ramp rate of 2.5 °C/min and kept for 12 h, followed by cooling at 2.5 °C/min to room temperature. The resulting powders of the second batch were found to melt at 580 °C with an applied pressure of 80 MPa for 30 min during hot pressing. The hot pressing temperature was then decreased to 540 °C/30 min with a ramp rate of 3 °C/min., followed by furnace cooling to room temperature.

As for the solid state reaction, high purity powders of bismuth oxide, copper powder, selenium powder were mixed and ground manually for 20 min. The resulting powders were then pressed into parallelepipeds. The pressed parallelepiped was then loaded into a Pyrex ampoule, which was evacuated using a diffusion pump to reach $10^{-5}$ to $10^{-6}$ Torr and then sealed. The parallelepiped in the encapsulated ampoule was then heated at 298 °C for 12 h and 580 °C for 24 h with a ramp rate of 3 °C/min followed by natural cooling to room temperature.

* Corresponding author.
*E-mail address:* liucj@cc.ncue.edu.tw (C.-J. Liu).

http://dx.doi.org/10.1016/j.scriptamat.2017.02.035
1359-6462/

Finally, the sample was hot pressed at 580 °C with an applied pressure of 80 MPa for 30 min followed by furnace cooling to room temperature. The details for characterization of samples and measurements of electrical resistivity, thermopower, thermal conductivity were described elsewhere [2–9,15–17].

## 3. Results and discussion

Fig. 1(a) shows the x-ray diffraction (XRD) patterns of the BiCuSeO samples synthesized by the conventional solid state reaction and the sol-gel method. The conventional solid state reaction sample (SSR) exhibits a single-phase (PDF # 45-0296), and no secondary phase is observed [12]. However, the sol-gel BiCuSeO sample shows the majority phase of BiCuSeO with the presence of a small amount of minor phases of $Bi_2O_3$ and $Bi_4Se_3$. It should be noted that there are several reports in the literature citing that minor impurity phases coexist with the majority phase of BiCuSeO [18,19,20]. The full width at half maximum (FWHM) of the most intense peak (102) is taken for evaluating the effects of synthesis on the BiCuSeO system. In all of the XRD patterns (Fig. 1a), the peak corresponding to the (1 0 2) plane occurring at around $2\theta = 38.0–38.6°$ is redrawn on an expanded scale shown in Fig. 1b. It is found that the FWHM is 0.143°, 0.194°, 0.165° for the SSR, SGA, and SGB, respectively, which corresponds to the average particle size of 95.14 nm, 111.864, 129.09 nm. The synthesis time of the sol-gel sample is much shorter (22 *h*) than that of the SSR. The refined lattice constants of BiCuSeO samples are $a = 3.9320(2)$ Å, 3.9320(1) Å, and 3.9287(3) Å, $c = 8.9373(5)$ Å, 8.9413(5) Å, 8.9313(2) Å for the SSR, SGA, and SGB, respectively. The lattice constants *a* and *c* of the BiCuSeO samples are in relatively good agreement with previous reports [12,21]. The bulk density is measured by applying the Archimedes principle at room temperature [22]. The bulk density of BiCuSeO is 6.83 g/cm$^3$, 8.09 g/cm$^3$ and 7.93 g/cm$^3$ for the SSR, SGA, and SGB, respectively, which corresponds to 77%, 92%, 90% of theoretical density. These values are in relatively good agreement with earlier report [23].

Fig. 2a and b shows the FE-SEM micrographs of fractured surfaces of BiCuSeO labelled as SSR and SGB. The micrograph of SSR yields larger grain sizes than that of SGB and the grains seem to be agglomerated. The TEM image in Fig. 2c shows the SGA's agglomerate of two or more particles, the particle sizes ranging from 75 to 120 nm, indicating the nanostructured nature of BiCuSeO sample synthesized by the sol-gel method. Fig. 2d shows the TEM image of SGA. The HRTEM image clearly exhibits a lattice fringes separated by a distance of 0.359 nm, 0.265 nm, 0.277 nm, corresponding to the interplanar distance of (101), (111), (110) planes of the tetragonal structure. The HRTEM image indicates nanostructured nature of sol-gel synthesized sample.

Table 1 summarizes the physical and transport properties of BiCuSeO at room temperature for the SSR, SGA, and SGB, respectively. The SSR sample shows the highest electrical resistivity among the samples. The electrical resistivity of SGA (0.027 Ω-cm) is lower than that of SGB (0.134 Ω-cm) at 300 K due to an increase in carrier concentration (Table 1). This further indicates that the synthesis procedure has dramatic effects on the electrical resistivity. The carrier concentration of BiCuSeO could be modified by either partial replacement of $Bi^{3+}$ by $M^{2+}$ in the insulating oxide $(Bi_2O_2)^{2+}$ layers, which induce holes to the conductive $(Cu_2Se_2)^{2-}$ layers, or introducing Cu-deficiency into the conductive $(Cu_2Se_2)^{2-}$ layers [12,24]. Liu et al. [25] reported that the $Bi_2O_3$ impurity is found in their Cu deficient $BiCu_{1-x}SeO$ samples with $x = 0.0$ to 0.1. Therefore, it is conceivable that there exists the Cu deficiency in our sol-gel samples in light of the presence of $Bi_2O_3$ impurity phase shown in the XRD patterns.

Fig. 3a shows the temperature dependence of electrical resistivity for BiCuSeO. It can be readily seen that the temperature dependence of SSR is different from that of the samples synthesized by the sol-gel method. The electrical resistivity of SSR decreases with increasing temperature, typical characteristic of nonmetal-like temperature dependence. However, the electrical resistivity of SGA and SGB increases with increasing temperature, a typical characteristic of metal-like temperature dependence. Fig. 3b shows the temperature dependence of thermopower for BiCuSeO. The positive thermopower confirms that the dominant charge carriers are holes for all the samples which is consistent with the Hall effect measurements. As seen in Table 1, when comparing the electrical resistivity and thermopower among the SSR, SSA, SSB and Li's BiCuSeO sample [12], the above statement is obeyed. Moreover, the thermopower of SSR sample and Li's sample increase with increasing temperature, a typical characteristic of metal-like temperature dependence. The thermopower of SGA exhibits a hump behavior. The thermopower of SGB monotonically decreases with increasing temperature, a typical characteristic of nonmetal-like temperature dependence.

The BiCuSeO system has two valence bands, that is, heavy and light valence bands. Nevertheless, the single parabolic band model has been adopted by several researchers for rough estimation of the effective mass of the BiCuSeO system [14,21,23,26]. In the present study we also adopt the single parabolic band model with the assumption that the acoustic phonon scattering is the dominant scattering mechanism

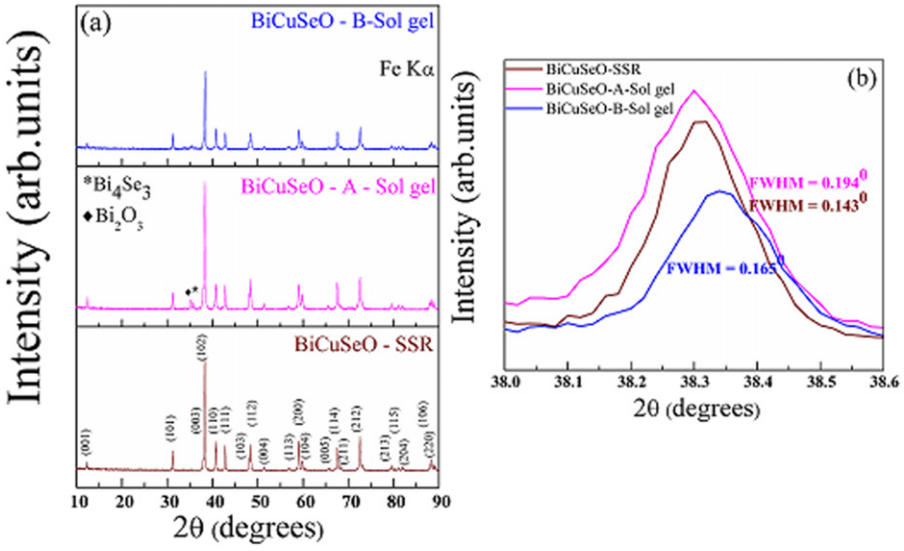


**Fig. 1.** (Color online) (a) Powder XRD patterns of the BiCuSeO (SSR: Solid State Reaction, sol-gel SGA sample, sol-gel SGB sample), (b) The peak at 38.0–38.6° in the XRD pattern (Fig. 1a) redrawn on an expanded scale to emphasize the intensity and FWHM of the peak (102). (For interpretation of the references to color in this figure legend, the reader is referred to the online version of this article.)